논문 12-37A-12-11

한국통신학회논문지 '12-12 Vol.37A No.12
http://dx.doi.org/10.7840/kics.2012.37A.12.1106

Application of 3GPP LTE and IEEE 802.11p Systems to Ship Ad-Hoc Network with the Existence of ISI

Xin Su◆, Bing Hui*, KyungHi Chang°, Gwangja Jin*

ABSTRACT

In order to provide high data rate and real time services under maritime environment, link-level performance of ship ad-hoc network (SANET) based on 3GPP LTE and IEEE 802.11p (WAVE) specifications are investigated and discussed in this paper. The measured maritime channel, whose delay spread is longer than the length of guard interval (GI) of both 3GPP LTE and IEEE 802.11p specifications, is adopted for the link-level simulations. For the purpose of eliminating inter-symbol interference (ISI) due to insufficient GI length, double antenna pattern (DAP) scheme and advanced time-domain decision-feedback equalizer (DFE) are proposed for LTE and WAVE systems, respectively. The proposed DFE removes the ISI in a same manner as the residual inter-symbol interference cancellation (RISIC) algorithm, but the inter-carrier interference (ICI) is reduced via cyclicity removal instead of cyclicity restoration used in the RISIC algorithm. Compared with existing schemes, our proposed DFE is a robust technique to overcome the severe ISI channel which has a comparatively large delay spread. Based on simulation results, not only comparisons between systems are discussed, but also some reformative suggestions are given.

Key Words : SANET, DFE, Cyclicity removal, Hard decision

Ⅰ. Introduction

Since the wireless networks over sea are not well developed as those over land, the existing communication systems over sea, such as Automatic Identification System (AIS), only provide low data rate non real-time services for ship identification, positioning, and email, etc.[1]. Also, the cost will be high for the services with the requirements of high data rate and low delay through satellite. Therefore, it is quite valuable to develop a new multi-hop maritime wireless network to provide higher data rate and real-time services. Ship Ad-hoc Network (SANET) has been proposed in [2] and [3] as a candidate multi-hop wireless communication system under the maritime environment.

Relatively low data rate is one of common problems in the existing maritime wireless networks. It not only limits the categories of services supported by maritime radio networks, but also the network architecture and coverage. For example, routing overheads for maritime networks must be kept as minimal as possible due to the extremely low data rate. Since that long-term evolution (LTE) specification [4] as defined by the third Generation Partnership Project (3GPP) and IEEE 802.11 specifications are highly flexible radio interfaces, in order to increase the data rate and robustness of the maritime communication system, advanced radio transmission technologies (RTT) such as orthogonal frequency division multiplexing (OFDM), based on

※ This work was supported by the IT R&D program of MKE/KEIT. [KI10038619, Development of Solution for Ship Safety Navigation based Maritime Ad-hoc Network].

◆ 주저자 : Department of Electronic Engineering, Inha University, leosu8622@hotmail.com, 정회원
° 교신저자 : Department of Electronic Engineering, Inha University, khchang@inha.ac.kr, 종신회원
* Department of Electronic Engineering, Inha University, huibing_zxo@163.com, 정회원
IT Convergence Technology Research Lab, Electronics and Telecommunications Research Institute, gjjin@etri.re.kr, 정회원

논문번호 : KICS2012-09-462, 접수일자 : 2012년 9월 27일, 최종논문접수일자 : 2012년 11월 20일

3GPP LTE and IEEE 802.11p specifications, can be employed for SANET.

IEEE 802.11p is an approved amendment to the IEEE 802.11 standard by supplementing wireless access in vehicular environments (WAVE) to support intelligent transportation systems (ITS) applications[5]. This includes data exchange between high-speed vehicles and the roadside infrastructure in the licensed ITS band of 5.9GHz (5.85-5.925GHz). 802.11p is used as the groundwork for dedicated short range communications (DSRC), which is an U.S. Department of Transportation project based on the ISO communications, air-interface, long and medium range (CALM) architecture standard. Particular applications of DSRC are toll collection, vehicle safety services, and commerce transactions via cars. The ultimate vision is a nationwide network that enables communications between vehicles and roadside access points or other vehicles. In this paper, link-level performance of two physical layers built by 3GPP LTE downlink and IEEE 802.11p (WAVE) are provided and analyzed, respectively. For the purpose of achieving acceptable system performance, suggestions and advanced receiver structures are given and proposed.

The remaining part of this paper is organized as follows. Overview of specifications is given in Section II, including basic physical (PHY) layer parameters in both 3GPP LTE and IEEE 802.11p specifications. In Section III, 2-path maritime channel modeling is described, and the proposed DFE along with the block diagram is explained in Section IV. The link-level simulation results of SANET with the PHY parameters of 3GPP LTE and WAVE are shown and discussed in Section V. Finally, conclusions are drawn in Section VI.

Ⅱ. Review of Specifications

2.1. 3GPP LTE (Release 8)

In 3GPP LTE downlink, total number of 4 transmit antennas are defined at the base station (BS), and maximum 2 codewords (CW) can be used [4]. In LTE downlink, after channel coding, interleaving and symbol mapping, the modulated data symbols are mapped to different layer(s). In the case of single codeword scheme, the modulated symbols from a single codeword are mapped to all the multiple-input multiple-output (MIMO) layers. For the case of a multi-codeword scheme where the number of codewords is equal to the number of MIMO layers, the one-to-one mapping between codewords and layers can be used in a straightforward manner. However, when the number of codewords is smaller than the number of MIMO layers, such as the case in the LTE systems for four antenna ports, the codewords to layer mapping follows the LTE specification[4]. In SANET system, the SISO transceiver structure with single codeword mapping is considered.

It is well known that the performance of a MIMO system can be improved with channel knowledge at the transmitter. In a time division duplex (TDD) system, the channel knowledge can be obtained at base station (BS) by uplink transmission through channel reciprocity. However, the sounding signals are required to be transmitted on the uplink, which imposes an additional overhead. In a frequency division duplex (FDD) system, the channel state information needs to be fed back from the user equipment (UE) to the BS. However, the complete channel state feedback can lead to excessive feedback overhead. An approach to reduce the channel state information feedback overhead is to use a codebook. For each transmission antenna configuration, a set of precoding matrices is constructed and known at both the BS and the UE. Once the codebook is specified for a MIMO system, the receiver observes a channel realization, selects the best precoding matrix to be used at the moment, and feeds back the precoding matrix index (PMI) to the transmitter.

After being precoded, the transmit symbols for each antenna port need to be mapped to physical resource elements (RE) and pass through the OFDM modulation process. Finally, these OFDM modulated symbols are fed into multiple physical antennas and sent into the radio channels. Fig.1 depicts resource to element mapping in one resource block. 2×2

pilot pattern is shown here as an example, where

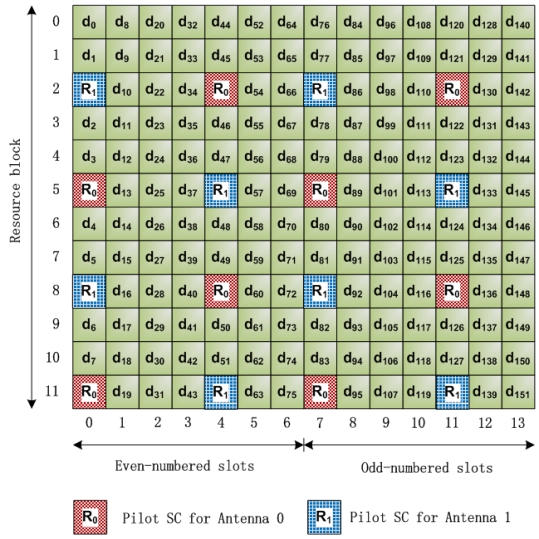

Fig. 1. Resource to element mapping in a resource block.

physical resource elements marked by "R_0" represent the pilot symbols for the first antenna and elements marked by "R_1" represent the pilot positions for the second antenna. In SISO system, only "R_0" positions are employed for pilot symbols, and we call this pilot pattern as single antenna pattern (SAP). On the other hand in 2 x 2 MIMO system, both "R_0" and "R_1" positions are employed for pilot symbols transmission, which is called double antenna pattern (DAP) in this paper. Though only single transmit antenna is assumed for SANET, we can employ both SAP and DAP into the SANET system for the purpose of performance comparison. It is obvious that pilot density of DAP is doubled than that of SAP, and channel estimation error based on DAP will be smaller. The details of frame structure and physical resource blocks can be found in [4].

2.2. IEEE 802.11p (WAVE)

The OFDM system in 802.11p provides a network with data payload communication capabilities of 6, 9, 12, 18, 24, 36, 48, and 54Mb/s. The support of transmitting and receiving at data rates of 6, 12, and 24Mb/s is mandatory[5]. Fig.2 illustrates baseband transceiver structure of the WAVE. In the figure, the source bits shall be coded by a convolutional encoder with the coding rate r = 1/2. The convolutional encoder uses the industry-standard generator polynomials of g_0 = 133 and g_1 = 171 with the constraints length of 7. Then, all encoded subcarriers are modulated by using BPSK, QPSK, 16 or 64 QAM. The frame structure of WAVE is shown in Fig.3. The preamble field consists of ten short symbols and two long symbols. Those ten short preambles are used for diversity selection, timing acquisition, and coarse frequency acquisition in the receiver. The two long preambles are used for channel estimation and fine frequency acquisition in the receiver. After preambles, the rate and length fields of the physical layer convergence procedure (PLCP) header are encoded by a convolutional code at a rate of r = 1/2, and are mapped onto a single OFDM symbol, denoted as the signal symbol.

In each OFDM symbol, four of the subcarriers are dedicated for pilot signals in order to make coherent detection robust against frequency offsets and phase noise. These pilot signals shall be put in subcarriers -21, -7, 7, and 21 as shown in Fig.3. After IFFT, cyclic prefix is extended to avoid ISI. At the receiver side, two long preambles are used to estimate channel condition [5], and the OFDM symbol is compensated by the channel estimation

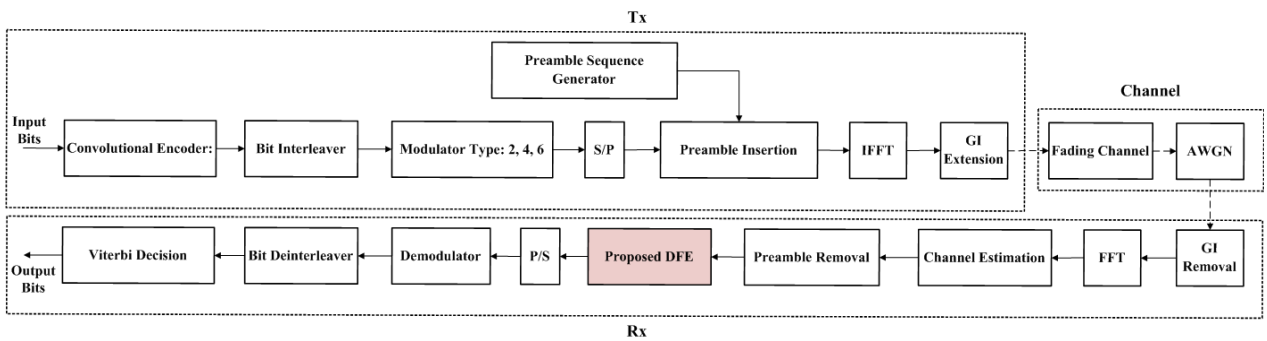

Fig. 2. WAVE transceiver structure.

results thereafter. Remaining parts perform the inverse operation of the transmitter. Note that, compared with LTE system, the GI (1.6 us) of WAVE system is relatively shorter than the one (4.7 us) of LTE system. Thus, an additional time-domain decision feedback equalizer (DFE) is proposed for WAVE to overcome the severe ISI. The shaded block in Fig.2 is the proposed time-domain DFE which will be explained in Section IV.

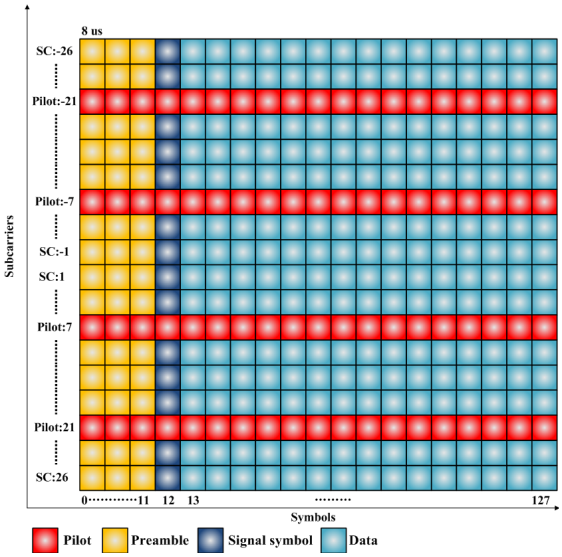

Fig. 3. WAVE frame structure.

Ⅲ. 2-path Maritime Channel Model

The maritime channel is modeled based on the measured channel delay profile given in[6]. The transmitter is located at sea shore with the height of 20 meters, and the receiver is located at boat which is 50 km far from the transmitter. The detailed channel parameters are shown in Table.1. The measurement scenario is coastline, where the channel environment is 2-path Rician fading channel composed of the first Rician distributed path and the second Rayleigh distributed path. The relative delay of the second path (Rayleigh distributed) is 5 us, and the power decay of it is 3 dB. The Rician *K*-factor is 10 dB. According to the maritime radio channel parameters in Table.1, the mathematical description of channel model is given as

$$g_{i,k}(t) = h_{i,k}^{Rician} + h_{i,k}^{Rayleigh} \quad (1)$$
$$= \sqrt{\frac{M}{M+1}}\left[\sqrt{\frac{K}{K+1}} + \sqrt{\frac{1}{K+1}}\, h_{i,k}^{1}(t)\right]\delta(t)$$
$$+ \sqrt{\frac{1}{M+1}}\, h_{i,k}^{2}(t)\delta(t-\tau)$$

where $h_{i,k}^{1}(t)$ and $h_{i,k}^{2}(t)$ are two independent Rayleigh paths. $h_{i,k}^{1}(t)$ is used to generate the Rician path ($h_{i,k}^{Rician}$) via the Richan *K*-factor. *M* is the normalization factor for two paths, and τ is the relative delay of the Rayleigh path.

Table. 1. 2-path maritime channel parameters.

Scenario	Cluster Index	Delay Spread (τ)	K	Average Relative Power (M)
Coastline	0	0 us	10 dB	3 dB
	1	5 us	0 dB	0 dB

Ⅳ. The Proposed Time-domain DFE for WAVE

Iterative techniques have been proposed in order to overcome the problem of GI insufficiency in [7-9]. The residual inter-symbol interference cancellation algorithm presented in [7], named by RISIC, is such a method, whose additional two steps are followed in the time domain. The first is to remove the residual ISI from the previously received OFDM symbol, and the second is to use reconstruction to restore the cyclicity in order to avoid the ICI. These two procedures are called tail cancellation and cyclicity reconstruction, respectively. Since we investigate a two-path fading channel, the procedure after the GI removal at the receiver for RISIC algorithm can be described by:

$$\hat{r}_{i,k} = r_{i,k} - r_{i|i-1,k} + \sum_{k=N-(C+G)+1}^{N} \hat{h}_{i,k}^{Rayleigh} x_{i,k} \quad (2)$$

where *N* represents the fast Fourier transform (FFT) size, *G* is the length of GI, and *C* is the value of (DS − GI). The residual ISI is removed from the received signal by subtracting the second term in (2), and the cyclicity is restored by the last term in

(2) in order to avoid ICI.

The RISIC algorithm presented in [7] has been shown to be most effective when the (DS − GI) difference is moderate. However, as the difference becomes larger, it cannot obtain a reliable estimation of the transmitted symbols in its initial step before the iteration, thereby causing degradation in performance. In [8], a reconstruction procedure of the cyclic prefix is proposed to efficiently restore the cyclicity of the *i*-th received symbol by adding the weighted (*i*+1)-th received symbol to the *i*-th received symbol. Hence, it can obtain a reliable estimation of the *i*-th transmitted symbol before the first iteration which mitigates the problem caused by an increased (DS − GI). The simulation results show that this procedure can maintain the system performance efficiently as the DS is incremented up to 55% of the symbol duration. However, several impractical assumptions are made in [8], including that the ISI removal is perfect, the estimated channel information is identical to the practical channel, and the noise is negligible. As is known, the ISI becomes severe with a DS increment, which leads to inaccurate symbol estimation. It is also known that the required signal for the cyclicity reconstruction of the *i*-th received symbol cannot be easily found in the first (DS − GI) samples, which is already severly affected by ISI, of the (*i*+1)-th received symbol. Therefore, we conclude that the *i*-th symbol cyclicity cannot be easily reconstructed by adding the weighted (*i*+1)-th received symbol to the *i*-th received symbol due to the severe ISI.

In this section, we suggest a new iterative scheme by modifying RISIC for the proposed DFE, which can work efficiently under severe ISI scenarios. Compared to the method found in [8], the proposed DFE is a more practical scheme that considers the ISI removal and noise. Fig.4 is the block diagram of the proposed DFE, where the modified blocks from RISIC are filled by color. Additionally, a perfect carrier and timing synchronization are assumed for the proposed DFE. The detailed procedure of the proposed DFE are described as follows:

1) Assume that the channel knowledge, i.e. DS, $\hat{h}_{i,k}^{Rayleigh}$ and $\hat{h}_{i,k}^{Rician}$, are perfectly known by receiver.

2) At the receiver, after the GI removal and FFT process, decisions regarding the transmitted samples $\{\hat{X}_{i-1,n}\}_{n=0}^{N-1}$ from symbol (*i*-1) are obtained for use in the tail cancellation. Of special note, the second long preamble in the time domain is directly used for $\{\hat{X}_{1,n}\}_{n=0}^{N-1}$ in tail cancellation. Then, $\{\hat{X}_{i-1,n}\}_{n=0}^{N-1}$ is converted back to the time domain by using IFFT, given as $\{\hat{x}_{i-1,k}\}_{k=0}^{N-1}$.

3) For the symbol of index *i*, the proposed DFE performs its tail cancellation by calculating the residual ISI and subtracts it from $\{r_{i,k}\}_{k=0}^{N-1}$ via

$$\hat{r}_{i,k}^{(0)} = r_{i,k} - \sum_{k=N+G-C+1}^{N} \hat{h}_i^{Rayleigh} \hat{x}_{i-1,k}, \qquad (3)$$

where "(0)" represents the state before the iteration.

4) The $\{\hat{r}_{i,k}^{(0)}\}_{k=0}^{N-1}$ obtained in Step 3 and $\hat{h}_{i,k}^{Rician}$ are converted to the frequency domain as $\{\hat{R}_{i,n}^{(0)}\}_{n=0}^{N-1}$ and $\hat{H}_{i,n}^{Rician}$, respectively.

5) Then, the zero forcing (ZF) strategy is used in the channel equalization (CE) to make the decisions on $\{\hat{X}_{i,n}^{(0)}\}_{n=0}^{N-1}$.

6) Afterwards, the decisions are converted back to the time domain as $\{\hat{x}_{i,k}^{(0)}\}_{k=0}^{N-1}$.

7) The ICI is generated by multiplying $\{\hat{x}_{i,k}^{(0)}\}_{k=0}^{N-1}$ and $\hat{h}_{i,k}^{Rayleigh}$, and the cyclicity removal is performed as

$$\hat{r}_{i,k}^{(I)} = \hat{r}_{i,k}^{(0)} - \sum_{k=N-G}^{N} \hat{h}_{i,k}^{Rayleigh} \hat{x}_{i,k}^{(I-1)} - \sum_{k=1}^{N-C} \hat{h}_{i,k}^{Rayleigh} \hat{x}_{i,k}^{(I-1)}, \qquad (4)$$

where *I* represents an iteration number with an initial value of *I* = 1. In (4), the second term represents the ICI which comes from the GI of symbol *i* when the cyclic prefix is used. The last term represents the ICI in the FFT interval for the symbol *i*, which comes from the delayed Rayleigh path.

8) Then, $\{\hat{r}_{i,k}^{(I)}\}_{k=0}^{N-1}$ is converted to the frequency domain as $\{\hat{R}_{i,n}^{(I)}\}_{n=0}^{N-1}$.

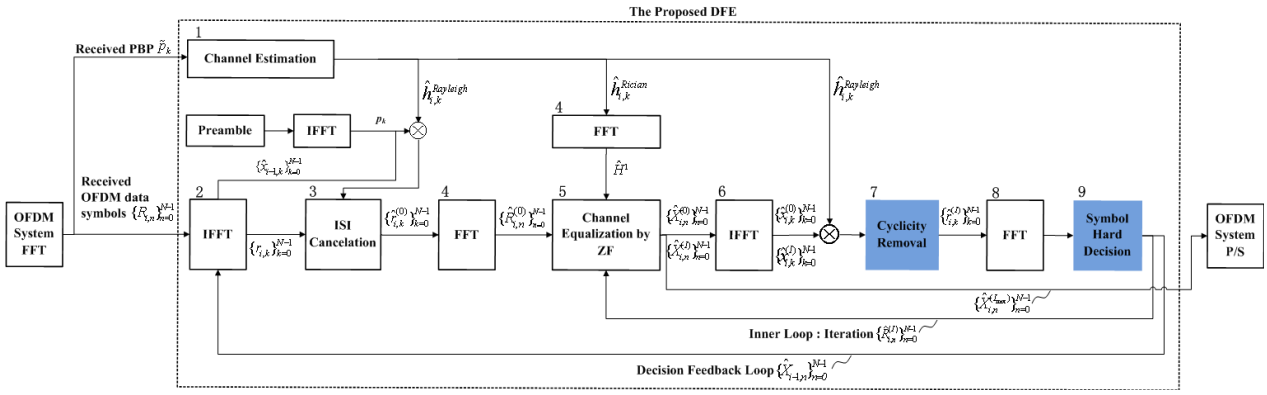

Fig. 4. The proposed DFE structure.

9) In Fig.4, the proposed symbol hard decision block in the frequency domain is aimed to determine $\{\hat{R}_{i,n}^{(I)}\}_{n=0}^{N-1}$ associated with correct constellation positions. The usage of hard decision prevents the outputs from the error propagations of which are fed back to the outer and inner loops. This block completes the *I*-th iteration in the proposed DFE.

10) For further iterations, convert $\{\hat{R}_{i,n}^{(I)}\}_{n=0}^{N-1}$ to $\{\hat{r}_{i,k}^{(I)}\}_{k=0}^{N-1}$, and repeat Steps 5 to 9 with *I* replaced by (*I* + 1). Note that, when the iteration is done, i.e. $I = I_{\max}$, the decisions $\{\hat{X}_{i,n}^{(I_{\max})}\}_{n=0}^{N-1}$ made by block 5 are the output of the proposed DFE, which will be forwarded to the P/S block of the OFDM system.

V. Simulation Results and Discussion

5.1. Link-level Performance of SANET by LTE

Table.2 shows the SANET system parameters adopted for link-level simulations. The carrier frequency is 2.075 GHz, and the maximum mobility of ships is assumed to be 30 Knots[10]. The system bandwidth is 10 MHz, which contains 600 data subcarriers (i.e., 50 physical resource blocks (PRBs)). The interleaver size is fixed as 5056 bits for the modulations of QPSK and 16 QAM, while 3008 bits is used for the modulation of 64 QAM. We consider the normal cyclic prefix (CP) of 73 samples (approximate 4.7us). In this case, small amount of inter symbol interference (ISI) may exist, but the high efficiency of system can be guaranteed compared with the case of extended CP. Moreover, the turbo coding along with the rate of r = 1/3 is used for all the modulation types.

Fig.5 and Fig.6 compare the simulation results with different modulation schemes employing different antenna patterns. When SAP is used, both bit error rate (BER) and packet error rate (PER) performances for all the modulation schemes are not acceptable. There are two reasons, where the first reason is the ISI due to the CP length of 4.7us is shorter than DS of 5us.

Table. 2. General parameters of SANET by LTE

Carrier Frequency	2.075 GHz
Bandwidth	10 MHz
Sampling Frequency	15.36 MHz
Subcarrier Spacing	15 kHz
FFT Size	1024
Nr. of Data Carriers	600
Effective OFDM Symbol Duration	66.667 *us*
GI Duration	≈ 5.2 *us* (1st OFDM Symbol) ≈ 4.7 *us* (2nd ~ 7th OFDM Symbols)
OFDM Symbol Duration	71.4196 *us*
Slot Duration	0.5 *ms*
Sub-frame Duration	1 *ms* (2 slots)
Frame Duration	10 *ms* (10 sub-frames)
Modulation	QPSK, 16 QAM, 64 QAM
Channel Coding	Turbo Coding (r = 1/3)

The second reason is the channel estimation error due to less pilot density when employing SAP. For comparison, DAP is additionally considered, and the simulation results are given in Fig.5, and in Fig.6 also. Obviously, when DAP is adopted, the performances are improved a lot, and they are acceptable except the results of 64 QAM. In the cases of QPSK and 16 QAM, DAP scheme can achieve the PER of 10^{-2} within 30 dB of Eb/N0.

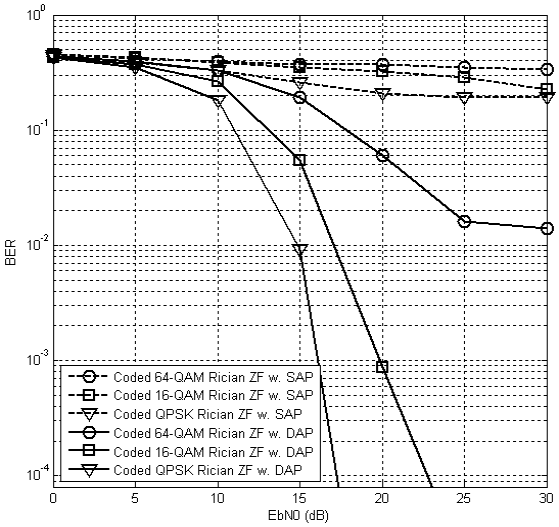

Fig. 5. BER results of LTE by employing different antenna patterns.

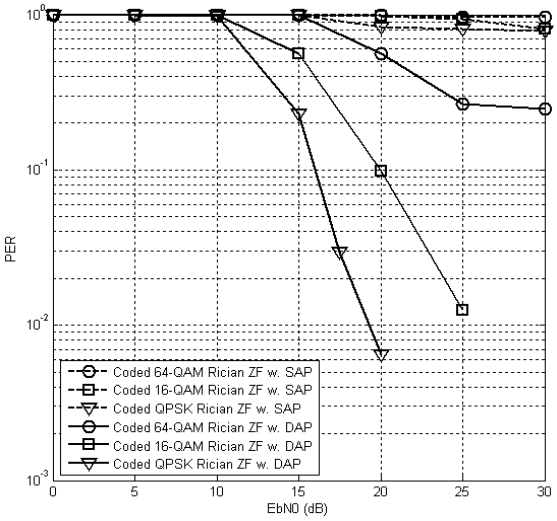

Fig 6. PER results of LTE by employing different antenna patterns.

However, channel estimation error and ISI seem to be still too severe for 64 QAM. Both BER and PER performances have the error floor, and never achieve the target BER and PER values.

5.2. Link-level Performance of SANET by WAVE

Table.3 gives the details of parameters for WAVE simulator, where carrier frequency and the maximum mobility are same with the LTE simulator. Since the length of WAVE packet is variable [1], we use two preambles and ten data symbols for each packet. Fig.7 gives the example which proves the poor BER is mainly due to the severe ISI. In Fig.7, in order

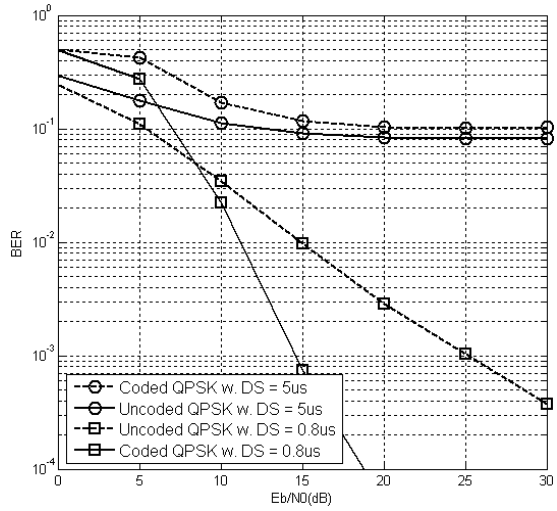

Fig. 7. BER results of WAVE by varying the value of delay.

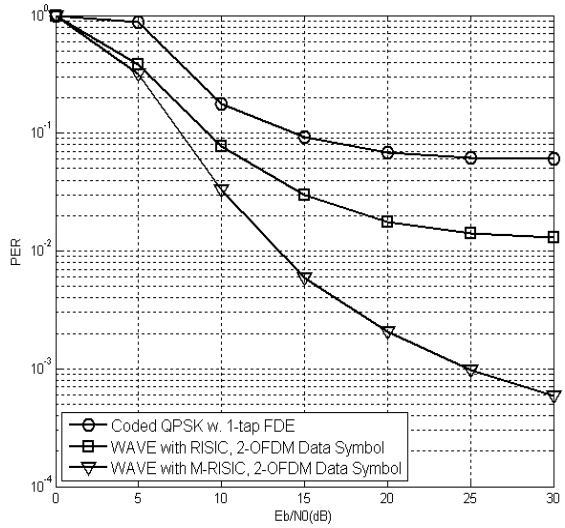

Fig. 8. PER results of WAVE with the proposed DFE.

to observe a fair comparison of the performance, we compare the case of 5 us DS (with ISI) with the case of 0.8 us (without ISI). The poor performance occurs when the DS of the second Rayleigh path is much longer, which is 5 us, than the GI (= 1.6 us). In addition, the coded BER is worse than uncoded BER, and no cross point exists within 30 dB. The reason is that the coding gain cannot be obtained under such a bad channel, but loss due to channel coding redundancy. However, when the DS value changes to 0.8 us, the obtained uncoded BER can reach to 10^{-3} after 25 dB, and almost 11 dB coding gain is obtained at the target BER of 10^{-3}.

Fig.8 shows the PER results of WAVE with the

proposed DFE. Based on Fig.8, we observe that WAVE with 1-tap frequency domain equalization (FDE) has the worst performance under severe ISI conditions. WAVE by using the DFE of RISIC algorithm yields more errors than the case of the proposed DFE. This is because RISIC algorithm cannot obtain a reliable estimation of the transmitted symbols via the cyclicity restoration instead of cyclicity removal used in the proposed DFE under severe ISI environment. According to Fig.8. WAVE with the proposed DFE can achieve the target PER of 10^{-3} at 30 dB. Note that, in this simulation, we use two preambles and two data symbols for each packet. When the frame length increases, the performance becomes worse due to the loss of accuracy since the current symbol is determined based on the previous one. Moreover, the performances are not acceptable for 16 QAM and 64 QAM even with the proposed DFE under the severe ISI channel.

Table. 3. General parameter of SANET by WAVE

Carrier Frequency	2.075 GHz
Bandwidth	10 MHz
Sampling Frequency	12.5 MHz
Subcarrier Spacing	156.25 kHz
FFT Size	64
Nr. of Data Carriers	48
Nr. of Virtual Carriers	11
Effective OFDM Symbol Duration	6.4 μs
GI Duration	1.6 μs
OFDM Symbol Duration	8 μs
Modulation Type	QPSK
Convolutional Coding	r = 1/2 Constraint Length : 7
Iteration Number (I) for DFE	2

Ⅵ. Conclusions

Physical layers of ship ad-hoc network (SANET) based on 3GPP LTE and IEEE 802.11p (WAVE) specifications are investigated and discussed in this paper. In 3GPP LTE system, due to ISI channel environment, DAP is used to obtain acceptable performances for QPSK and 16 QAM modulations. However, even with DAP, 64 QAM cannot be employed due to its low robustness against ISI and channel estimation error. For IEEE 802.11p, because of the severe ISI, we propose the novel time-domain DFE by modifying the algorithm of RISIC. The performances with the modulation of QPSK can achieve the target performance with the proposed DFE. According to our simulation results, we conclude that the 3GPP LTE system can achieve an acceptable system performance with simple modification, i.e., DAP scheme. However, for the WAVE system, a complex DFE receiver structure is required under the severe ISI channel.

References

[1] *Technical clarifications of recommendation ITU-R M.1371-1, Technical characterisitcs for a universal shipborne automatic identification system using time division multiple access in the VHF maritime mobile band*, 1.5 Ed., 2004.

[2] Y. B. Kim, J. H. Kim, Y. P. Wang, K. H. Chang, J. W. Park, and Y. K. Lim, “Application scenarios of nautical ad-hoc network for maritime communications,” in *Proc. IEEE Oceans-Fall*, Bremen, Germany, Oct. 2009.

[3] K. H. Jeon, B. Hui, K. H. Chang, S. G. Kim, S. M. Kim, and Y. K. Lim, “Performance analysis of channel compensation and channel coding techniques based on measured maritime wireless channel in VHF-band ship ad-hoc network,” *J. KICS*, vol. 36, no. 5, pp. 517-529, May 2011.

[4] *3GPP TS 36.211* (8.6.0), *Evolved universal terrestrial radio access (E-UTRA): physical channels and modulation*, Mar. 2009.

[5] *IEEE Standard. 802.11p TM-2010, Amendment 6: Wireless access in vehicular environments*, Jul., 2010.

[6] *ETSI TR 102 580 (V1.1.1), Technical report : Terrestrial trunked radio (TETRA), Designer’s guide, TETRA high-speed data (HSD), TETRA enhanced data service (TEDS), Rel-2*, Oct. 2007.

[7] D. Kim and G. L. Stuber, “Residual ISI Cancellation for OFDM with application to

HDTV broadcasting," *IEEE J. Sel. Areas Comm.*, vol. 16, no. 8, pp. 1590-1599, Oct. 1998.

[8] C. Park and G. Im, "Efficient cyclic prefix reconstruction for coded OFDM systems," *IEEE Commun. Lett.*, vol. 8, no. 5, pp. 274-276, May 2004.

[9] Z. Yang, W. Bai, and Z. Liu, "A decision-aided residual ISI cancellation algorithm for OFDM systems," in *Proc. Int. Conf. Signal Proc. (ICSP)*, pp. 20-23, Guilin, China, Nov. 2006.

[10] K. Yang, T. Roste, F. Bekkadal, and T. Ekman, "Channel characterization including path loss and Doppler effects with sea reflections for mobile radio propagation over sea at 2GHz," in *Proc. Wireless Commun. and Signal Proc. (WCSP)*, pp. 1-6, Suzhou, China, Oct. 2010.

소 신 (Xin Su)

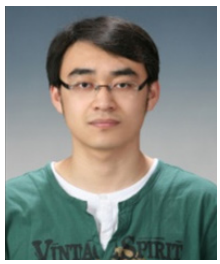

2008년 7월 중국 쿤민이공대학교 컴퓨터공학과 공학사
2010년 8월 조선대학교 컴퓨터공학과 공학석사
2011년~현재 인하대학교 정보통신 대학원 박사과정
<관심분야> Mobile Ad-hoc Network, OFDM/ MIMO

휘 빙 (Bing Hui)

2005년 7월 중국 동북대학교 정보통신공학과 (공학사)
2009년 8월 인하대학교 정보통신 대학원 (공학석사)
2009년~현재 인하대학교 정보통신 대학원 박사과정
<관심분야> OFDM/MIMO, MIMO Detection, 3GPP LTE

장 경 희 (KyungHi Chang)

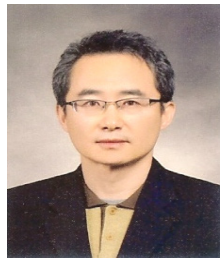

1985년 2월 연세대학교 전자공학과 공학사
1987년 2월 연세대학교 전자공학과 공학석사
1992년 8월 Texas A&M Univ., EE Dept. (Ph.D.)
1989년~1990년 삼성종합기술원 주임연구원
1992년~2003년 한국전자통신연구원, 이동통신연구소 무선전송방식연구팀장, 책임연구원
2003년~현재 인하대학교 전자공학과 교수
<관심분야> 3GPP LTE 및 WMAN 무선전송방식, Corss-layer Design, Cooperative Relaying System, Cognitive Radio, RFID/USN Systems, Mobile Ad-hoc Network, 해상통신, 편파안테나 무선전송방식 등

진 광 자 (Gwangja Jin)

1987년 2월 건국대학교 전자공학과 공학사
1990년 2월 건국대학교 전자공학과 공학석사
1990년 2월~현재 한국전자통신연구원 책임연구원
<관심분야> 위성통신, 센서네트워크, 조선/해양 IT